



You have downloaded a document from  
**RE-BUŚ**  
repository of the University of Silesia in Katowice

**Title:** Tribological properties of Ti-6Al-7Nb alloy after isothermal oxidation

**Author:** Krzysztof Aniołek, Adrian Barylski, Denis Osior

**Citation style:** Aniołek Krzysztof, Barylski Adrian, Osior Denis. (2019). Tribological properties of Ti-6Al-7Nb alloy after isothermal oxidation. "Tribologia" (Nr 3 (2019), s. 5-12), doi 10.5604/01.3001.0013.5428



Uznanie autorstwa - Na tych samych warunkach - Licencja ta pozwala na kopiowanie, zmienianie, rozprowadzanie, przedstawianie i wykonywanie utworu tak długo, jak tylko na utwory zależne będzie udzielana taka sama licencja.



UNIwersytet ŚLĄSKI  
W KATOWICACH



Biblioteka  
Uniwersytetu Śląskiego



Ministerstwo Nauki  
i Szkolnictwa Wyższego

Krzysztof ANIOŁEK\*, Adrian BARYLSKI\*\*, Denis OSIOR\*\*\*

## TRIBOLOGICAL PROPERTIES OF Ti-6Al-7Nb ALLOY AFTER ISOTHERMAL OXIDATION

### WŁAŚCIWOŚCI TRIBOLOGICZNE STOPU Ti-6Al-7Nb PO UTLENIANIU IZOTERMICZNYM

**Key words:**

thermal oxidation, surface morphology, oxide layers, tribological properties.

**Abstract**

The paper presents the characterization of tribological properties of the Ti-6Al-7Nb alloy before and after isothermal oxidation in different friction couples. Microscopic observations have shown that uniform oxide layers were obtained, which evenly covered the entire surface of the investigated samples. It was found that oxide layers deposited on the Ti-6Al-7Nb alloy substrate contribute to a considerable improvement of the tribological properties. The best resistance to sliding wear was shown by the layer obtained at a temperature of 600°C. It was also shown that presence of oxide layers on the surface of the Ti-6Al-7Nb alloy leads to an increase in the friction coefficient. The highest increase in the value of the friction coefficient was observed for a surface oxidized at 650°C during interaction with an Al<sub>2</sub>O<sub>3</sub> ball. SEM observations of traces of the tribological interaction showed the presence of numerous scratches and fine wear products on the friction surface. For the non-oxidized condition, after interaction with a ball made of bearing steel 100Cr6, the presence was found of alternating, morphologically varied areas which had formed as a result of corrugation wear. Tests have shown that isothermal oxidation eliminates this disadvantageous phenomenon.

**Słowa kluczowe:**

utlenianie izotermiczne, morfologia powierzchni, warstwy tlenkowe, właściwości tribologiczne.

**Streszczenie**

W pracy przedstawiono charakterystykę właściwości tribologicznych stopu Ti-6Al-7Nb przed oraz po utlenianiu izotermicznym w różnych skojarzeniach ciernych. Obserwacje mikroskopowe wykazały, że otrzymano jednolite warstwy tlenkowe, które równomiernie pokrywały całą powierzchnię badanych próbek. Stwierdzono, że warstwy tlenkowe otrzymane na podłożu stopu Ti-6Al-7Nb prowadzą do znacznej poprawy właściwości tribologicznych. Najlepszą odpornością na zużycie ściernie cechowała się warstwa tlenkowa otrzymana w temperaturze 650°C. Wykazano ponadto, że obecność warstw tlenkowych na powierzchni stopu Ti-6Al-7Nb prowadzi do wzrostu współczynnika tarcia. Największy wzrost współczynnika tarcia zaobserwowano dla powierzchni utlenionej w temperaturze 650°C podczas współpracy z kulką Al<sub>2</sub>O<sub>3</sub>. Obserwacje SEM śladów współpracy tribologicznej wykazały na powierzchni tarcia obecność licznych rys oraz drobne produkty zużycia. Dla stanu nieutlenionego po współpracy z kulką ze stali łożyskowej 100Cr6 stwierdzono obecność naprzemianległych różnych morfologicznie obszarów powstałych w wyniku zużycia falistego. Wykazano, że utlenianie izotermiczne eliminuje to niekorzystne zjawisko.

## INTRODUCTION

Titanium and its alloys belong to materials widely used in technical and biomedical engineering. Over the past years, a growing interest has been observed in these materials, inter alia, in the aircraft, space, chemical, ship

building, military, and power engineering industries, as well as in implantation, which results mainly from the unique combination of their mechanical properties (a high strength to density ratio), exceptional corrosion resistance, and perfect biocompatibility [L. 1–3].

\* ORCID: 0000-0002-5382-2038. University of Silesia, Institute of Materials Science, 75 Pułku Piechoty 1A Street, 41-500 Chorzów, Poland.

\*\* ORCID: 0000-0002-1863-1471. University of Silesia, Institute of Materials Science, 75 Pułku Piechoty 1A Street, 41-500 Chorzów, Poland.

\*\*\* University of Silesia, Institute of Materials Science, 75 Pułku Piechoty 1A Street, 41-500 Chorzów, Poland.

Pure titanium is characterized by the best biocompatibility among metallic materials, but, at the same time, it has low strength and poor tribological properties, which are a significant cause of damage to the surface layer and often results in toxic products of wear penetrating into the human body [L. 4]. In addition, the mechanical properties of titanium are often insufficient in a number of technical or biomedical applications where there is a necessity to carry increased loads. Significant improvement of mechanical properties and corrosion resistance can be achieved by introducing alloying additions to titanium, which allows obtaining a material with much better strength and corrosion characteristics. Alloying additions, such as aluminium and vanadium, improve the functional properties of titanium alloys, but often worsen their biocompatibility [L. 4, 5]. One way to eliminate these problems is to use surface engineering methods. Such an approach allows the creation of new areas of potential applications for modified titanium and its alloys and, at the same time, allows increasing the wear resistance, while maintaining other specific properties of the material.

Titanium is a highly reactive metal, which, when exposed to the environment, reacts with oxygen to form an oxide layer several nanometres thick, which reduces further oxidation and oxygen diffusion at lower temperatures. However, in their natural form, TiO<sub>2</sub> layers have poor mechanical properties and crack easily under conditions of frictional corrosion and sliding friction [L. 6, 7]. Long-term dissolution of exposed metal after breaking the continuity of the passive oxide layer results in a gradual wear of the material.

Isothermal oxidation is a method that takes advantage of the high affinity of oxygen with titanium, which allows increasing the resistance to sliding wear through an oxygen diffusion-hardened upper layer, with the latter having very good tribological properties. This method makes it possible to obtain oxide layers with a varied phase composition and functional properties. The roughness of the oxidized surface can also be controlled by selecting appropriate oxidation parameters. The results of previous research clearly indicate that isothermal oxidation may be a more effective method for increasing resistance to sliding wear than ion nitriding [L. 8].

The purpose of this study is to determine the influence of different friction couples (Al<sub>2</sub>O<sub>3</sub>, ZrO<sub>2</sub> and bearing steel 100Cr6) on the tribological properties of the Ti-6Al-7Nb alloy after isothermal oxidation at temperatures of 600, 650, and 700°C. The surface morphology of oxide layers, volumetric wear, and the friction coefficient have been determined and an analysis of the traces of wear has been conducted using scanning electron microscopy.

## EXPERIMENTAL PROCEDURES

Ti-6Al-7Nb alloy, which is widely used in medicine due to its low density and excellent corrosion resistance, was used in the research. The most popular applications for

the alloy are artificial hip joints, spine stabilizers, and dental implants. Parameters of the oxidation of Ti-6Al-7Nb alloy were selected based on the previous results of the authors' research presented in paper [L. 9]. As part of the research, oxidation was conducted for periods of 20 minutes to 72 hours, at temperatures of 500, 600, 700, 800, and 900°C. On the basis of the obtained results, it was found that oxidation conducted at 500°C did not result in an increase in the mass of the specimen in the analysed time frame of the oxidation process. At the same time, the oxide layers obtained at 900°C were characterized by poor adhesion and susceptibility to flaking and spalling. Based on the obtained results, it was found that the most optimal solution would be oxidation of the Ti-6Al-7Nb alloy at temperatures of 600°C, 650°C, and 700°C for a period of 72 h, which would allow obtaining diversified morphologies and thicknesses of the oxide layers obtained, while ensuring their good quality.

Observation of the surface morphology of the oxide layers obtained on Ti-6Al-7Nb alloy was conducted using a JEOL JSM 6480 scanning electron microscope. The observations were carried out at a magnification of 1000x on specimens oxidized at 600°C, 650°C, and 700°C for 72 h.

Tribological tests were performed under constant measurement conditions using a tribological tester, TRN Tribometer (Anton Paar, Switzerland), operating in the ball-on-disc system in rotary motion. The tester was used to determine the volumetric wear and friction coefficient of the friction couple. Tribological tests were repeated 3 times each at a temperature of 21±1°C and a humidity of 40±5%. The specimens were 40 mm diameter discs made of the Ti-6Al-7Nb alloy and 6 mm diameter balls made of aluminium oxide, and zirconium oxide and bearing steel (100Cr6) served as counter-specimens. The tests were performed in the following conditions:

- Load –  $F = 5$  N,
- Linear velocity –  $v = 0.1$  m/s,
- Friction distance –  $s = 1000$  m.

After tribological tests, the volumetric wear was determined for discs made of Ti-6Al-7Nb alloy subjected and not subjected to isothermal oxidation. Registration of wear trace profiles was performed using a Mitutoyo SJ-500 contact profilometer. Volumetric wear was calculated from the following formula:

$$V_v = \frac{V}{F \cdot s} \quad (1)$$

where

$V_v$  – volumetric wear [mm<sup>3</sup>/N·m],

$V$  – volume of the material removed during friction [mm<sup>3</sup>],

$F$  – load [N],

$s$  – friction distance [m].

The morphology of the friction surface on the Ti-6Al-7Nb alloy after a tribological interaction with  $\text{Al}_2\text{O}_3$ ,  $\text{ZrO}_2$ , and 100Cr6 balls was observed on a JEOL JSM-6480 scanning electron microscope.

## RESULTS AND DISCUSSION

### Surface morphology of oxide layers

Figures 1–3 present microscopic images of the surface morphology of Ti-6Al-7Nb alloy after 72 hours of isothermal oxidation at 600°C, 650°C, and 700°C.

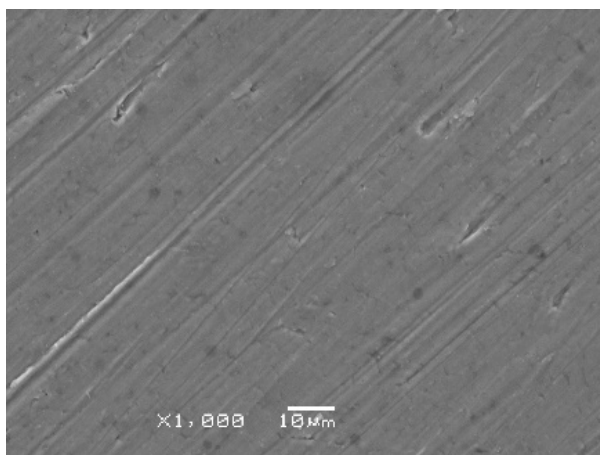


**Fig. 1. Surface morphology of the oxide layer obtained at a temperature of 600°C in time of 72 h**

Rys. 1. Morfologia powierzchni warstwy tlenkowej otrzymanej w temperaturze 600°C w czasie 72 h

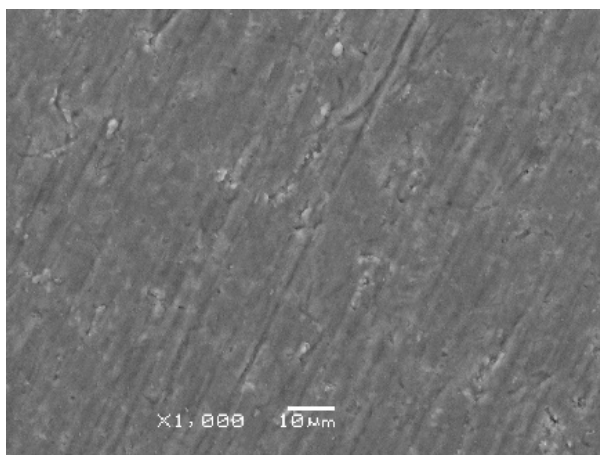


**Fig. 2. Surface morphology of the oxide layer obtained at a temperature of 650°C in time of 72 h**

Rys. 2. Morfologia powierzchni warstwy tlenkowej otrzymanej w temperaturze 650°C w czasie 72 h

An analysis of microscopic images showed that uniform oxide layers were obtained, which evenly covered the surface of the Ti-6Al-7Nb alloy. No signs of scale spalling or coming off were observed. On the surface covered with oxide layers, scratches were visible which had formed during grinding of the samples for

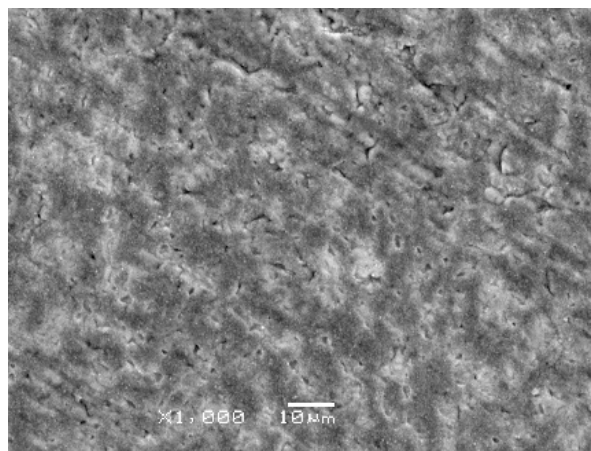


**Fig. 3. Surface morphology of the oxide layer obtained at a temperature of 700°C in time of 72 h**

Rys. 3. Morfologia powierzchni warstwy tlenkowej otrzymanej w temperaturze 700°C w czasie 72 h

tribological tests, which testified to the low thickness of the oxide layer. The direction of the scratches was particularly noticeable at temperatures of 600°C and 650°C; whereas, at 700°C, this phenomenon did not occur, which means that the deposited oxide layer had a thickness sufficient to cover scratches formed after grinding.

On the basis of the observations, it was found that the surface morphology of the obtained oxide layers varied, depending on the oxidation temperature. It was also found that the size of oxide particles increased with an increasing oxidation temperature, which is particularly noticeable after oxidation at the temperature of 700°C. In that case, the obtained layer was characterized by agglomerations of fine oxide particles, which formed local thickenings on the surface. Simultaneously, the occurrence of fine craters was detected in the oxide layer. A similar morphology was obtained in paper [L. 1] after the oxidation of Ti-6Al-4V alloy at 700°C for 4–8 h. The authors of paper [L. 10] have found that small grains of titanium oxide are formed as a result of the agglomeration of oxide particles.

### Tribological properties of oxide layers formed on the Ti-6Al-7Nb alloy

Figure 4 presents the results of volumetric wear after tribological tests of the Ti-6Al-7Nb alloy in the non-oxidized and oxidized condition, depending on the tribological couple used ( $\text{Al}_2\text{O}_3$ ,  $\text{ZrO}_2$ , 100Cr6).

Analysis of the obtained results showed that presence of oxide layers significantly improves the tribological properties of the Ti-6Al-7Nb alloy, which is directly connected with an increase in the surface hardness after oxidation [L. 1]. The greatest volumetric wear occurred for a disc made of Ti-6Al-7Nb in the non-oxidized condition, during an interaction with each of

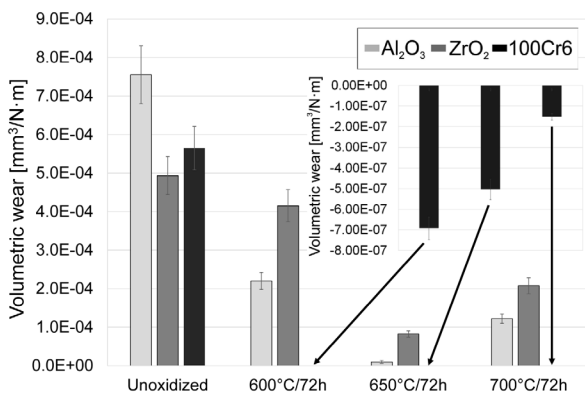


**Fig. 4. Volumetric wear of a disc made of Ti-6Al-7Nb alloy in the non-oxidized and oxidized condition, depending on the friction couple**

Rys. 4. Zużycie objętościowe tarczy ze stopu Ti-6Al-7Nb w stanie nieutlenionym oraz utlenionym w zależności od skojarzenia ciernego

the counter-specimens. In particular, the highest wear was found after an interaction with an Al<sub>2</sub>O<sub>3</sub> ball, whose hardness was the highest of all the materials used, while the friction couple Ti-6Al-7Nb-ZrO<sub>2</sub> showed the lowest wear. The wear after interaction with the 100Cr6 bearing steel was found to be a little higher compared to that after interaction with the ZrO<sub>2</sub> ball.

After isothermal oxidation of Ti-6Al-7Nb alloy, a reduction was observed in the volumetric wear, which depended on the oxidation temperature and the friction couple. Tribological interaction of the oxide layer obtained at 600°C with the Al<sub>2</sub>O<sub>3</sub> ball resulted in more than a triple reduction in volumetric wear. For the ZrO<sub>2</sub> ball, the wear decreased by ca. 16%. After oxidation of the Ti-6Al-7Nb alloy at 650°C, a further reduction of the volumetric wear was observed. During the tribological interaction of a disc oxidized at 650°C with an Al<sub>2</sub>O<sub>3</sub> ball, the greatest reduction in the volumetric wear was observed (more than 98%). Tribological tests performed with the ZrO<sub>2</sub> ball showed a little higher wear (a wear reduction by 83%). The increase in the resistance to sliding wear was caused by higher intensity of the oxidation process, which was related to the fact that the obtained oxide layer was thicker and had a higher hardness [L. 11]. At the same time, after oxidation at a temperature of 700°C, a slightly increased wear was once again observed, which may have been connected with the deterioration of adhesion of the obtained oxide layer. Completely different tribological characteristics were obtained during interaction of the Ti-6Al-7Nb alloy with bearing steel grade 100Cr6. Both after oxidation at temperatures of 600°C and 650°C, and at 700°C, no traces of sliding wear were found (Fig. 4). On the basis of profilometric measurements and microscopic observations (detailed results are presented later in

the paper), it was shown that during a tribological interaction between the oxidized disc and bearing steel 100Cr6, the working surface of friction was oxidized. The observed phenomenon resulted in an increase in the material on the trace of friction (Fig. 7), which is visible in Fig. 4 in the form of a negative value of volumetric wear.

Figures 5–7 present examples of the wear trace profiles obtained after tribological tests on the Ti-6Al-7Nb disc oxidized at a temperature of 700°C. In the case of interaction with ceramic balls (Al<sub>2</sub>O<sub>3</sub> and ZrO<sub>2</sub>), the presence of characteristic wear traces was found. Their geometry depended on the material of the counter-specimen used. After interaction with the Al<sub>2</sub>O<sub>3</sub> ball, a wear trace in the form of deep scratches was found on the surface of the disc. In the case of the ZrO<sub>2</sub> counter-specimen, a semi-circular trace with gentle scratches was obtained. After interaction with the 100Cr6 ball, no wear was found. At the same time, an increase in the material was observed on the wear trace (Fig. 7).

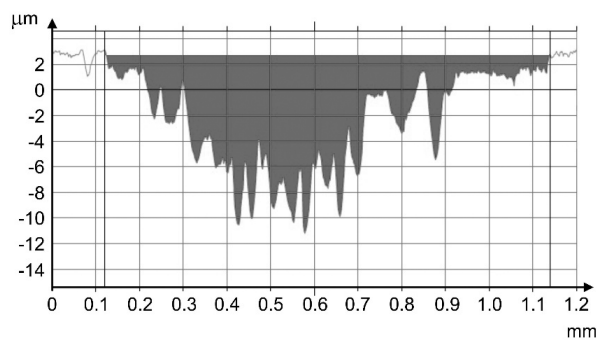


**Fig. 5. Example profile of a friction trace on a disc oxidized at 700°C after interaction with an Al<sub>2</sub>O<sub>3</sub> ball**

Rys. 5. Przykładowy profil śladu tarcia na tarczy utlenionej w temperaturze 700°C po współpracy z kulką Al<sub>2</sub>O<sub>3</sub>

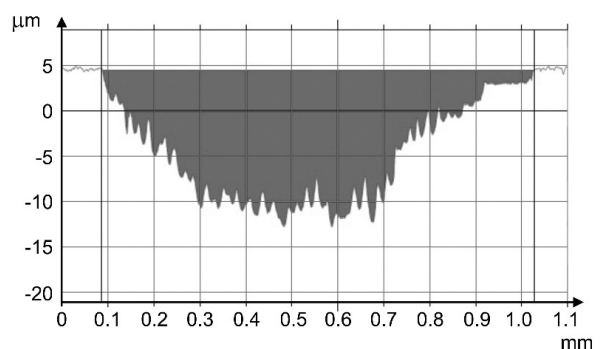


**Fig. 6. Example profile of a friction trace on a disc oxidized at 700°C after interaction with a ZrO<sub>2</sub> ball**

Rys. 6. Przykładowy profil śladu tarcia na tarczy utlenionej w temperaturze 700°C po współpracy z kulką ZrO<sub>2</sub>

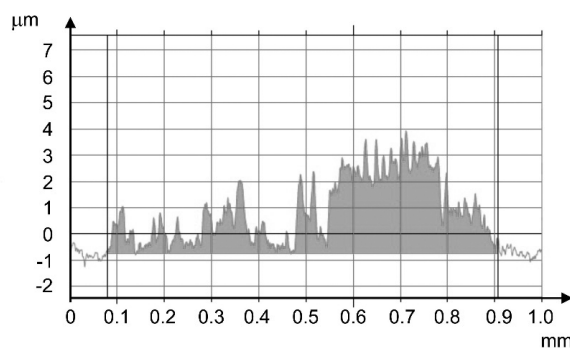


Fig. 7. Example profile of a friction trace on a disc oxidized at 700°C after interaction with a 100Cr6 bearing steel ball

Rys. 7. Przykładowy profil śladu tarcia na tarczy utlenionej w temperaturze 700°C po współpracy z kulką ze stali łożyskowej 100Cr6

### Friction coefficient

Figure 8 presents a juxtaposition of the mean value of friction coefficient during a tribological interaction of a non-oxidized and oxidized disc made of the Ti-6Al-7Nb alloy with  $\text{Al}_2\text{O}_3$ ,  $\text{ZrO}_2$ , and 100Cr6 balls.

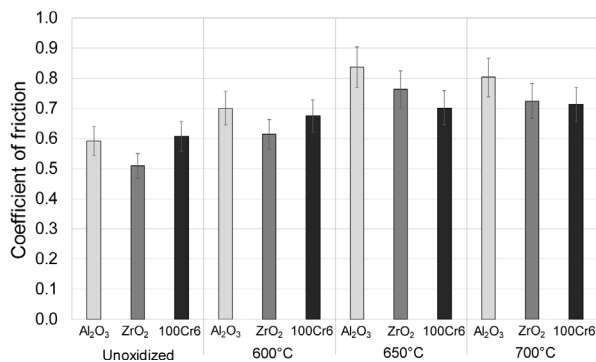


Fig. 8. Stabilized friction coefficient during a tribological interaction of the Ti-6Al-7Nb alloy with  $\text{Al}_2\text{O}_3$ ,  $\text{ZrO}_2$ , and 100Cr6 balls

Rys. 8. Ustabilizowany współczynnik tarcia podczas współpracy tribologicznej stopu Ti-6Al-7Nb z kulkami  $\text{Al}_2\text{O}_3$ ,  $\text{ZrO}_2$  oraz 100Cr6

Based on the analysis of test results, it was found that the lowest values of the friction coefficient were obtained for the non-oxidized surface. During the interaction with  $\text{Al}_2\text{O}_3$  and 100Cr6 balls, the friction coefficient reached a value of approximately  $\mu = 0.6$ . The lowest friction coefficient was obtained for the couple with a  $\text{ZrO}_2$  ball (ca.  $\mu = 0.5$ ). After isothermal oxidation, an increase in the friction coefficient value was observed, which is a result different than those found among some published data [L. 1, 12]. After oxidation at 600°C, the friction coefficient increased by ca. 0.1 and, similarly to the non-oxidized surface, its lowest value was obtained for the  $\text{ZrO}_2$  ball. After oxidation at temperatures of 650°C and 700°C, a further increase in the friction coefficient value was observed. The tribological interaction with the oxide

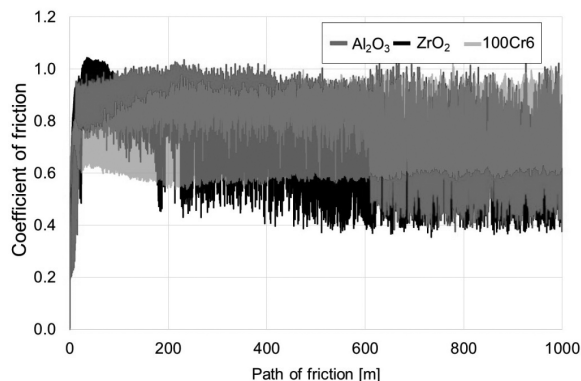


Fig. 9. Example of changes in the friction coefficient after oxidation at 700°C, depending on the counter-specimen used

Rys. 9. Przykładowy przebieg współczynnika tarcia po utlenianiu w temperaturze 700°C w zależności od zastosowanej przeciwpróbki

layer obtained at 650°C led to the highest values of the friction coefficient, especially during interaction with the  $\text{Al}_2\text{O}_3$  ball (ca.  $\mu = 0.84$ ). The interaction between the disc and  $\text{ZrO}_2$  and 100Cr6 balls also resulted in a friction coefficient of an increased value ( $\mu = 0.76$  and  $\mu = 0.7$ , respectively). Similar values of the friction coefficient were also obtained for the oxide layers deposited at the temperature of 700°C. The increase in the friction coefficient may be caused by the increased surface roughness after oxidation [L. 13].

As part of tribological tests, the course of changes in the friction coefficient was also determined, depending on the friction distance covered and the type of counter-specimen. Example results for the Ti-6Al-7Nb disc oxidized at 700°C are presented in Fig. 9. During the tribological interaction of an oxide layer with the  $\text{Al}_2\text{O}_3$  ball, the stabilized friction coefficient reached ca. 0.9. However, after exceeding the friction distance of 600 m, its amplitude significantly widened, which may be connected with the wear through the oxide layer and further tribological interaction with the substrate. In the tests with  $\text{ZrO}_2$  and 100Cr6 balls, no similar phenomenon was observed. The tests with the  $\text{ZrO}_2$  ball showed that, after reaching a stabilized value (ca. 0.7), the friction coefficient remained at a similar level until the end of the tests. Its amplitude was found to be higher than in the tests with the  $\text{Al}_2\text{O}_3$  ball. The most stable friction coefficient (ca. 0.75), with a lower amplitude compared to the tests with the  $\text{ZrO}_2$  ball, was obtained during the tribological interaction between the Ti-6Al-7Nb disc and a ball made of the 100Cr6 bearing steel.

### Surface morphology of wear traces after tribological tests

Figures 10–14 show the results of microscopic observation of the working surface of friction on non-oxidized samples and on samples oxidized at temperatures of 600°C, 650°C, and 700°C.

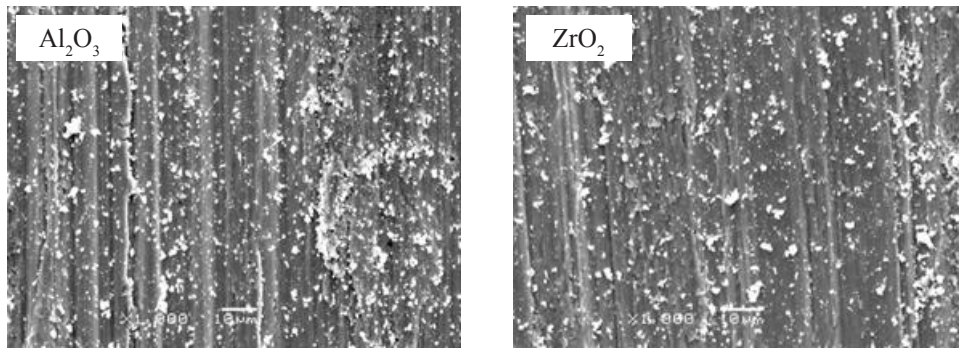


**Fig. 10. Surface of the wear trace on Ti-6Al-7Nb samples in the non-oxidized condition after interaction with  $\text{Al}_2\text{O}_3$  and  $\text{ZrO}_2$  balls**

Rys. 10. Powierzchnia śladu zużycia na próbkach ze stopu Ti-6Al-7Nb w stanie nieutlenionym po współpracy z kulkami  $\text{Al}_2\text{O}_3$  oraz  $\text{ZrO}_2$

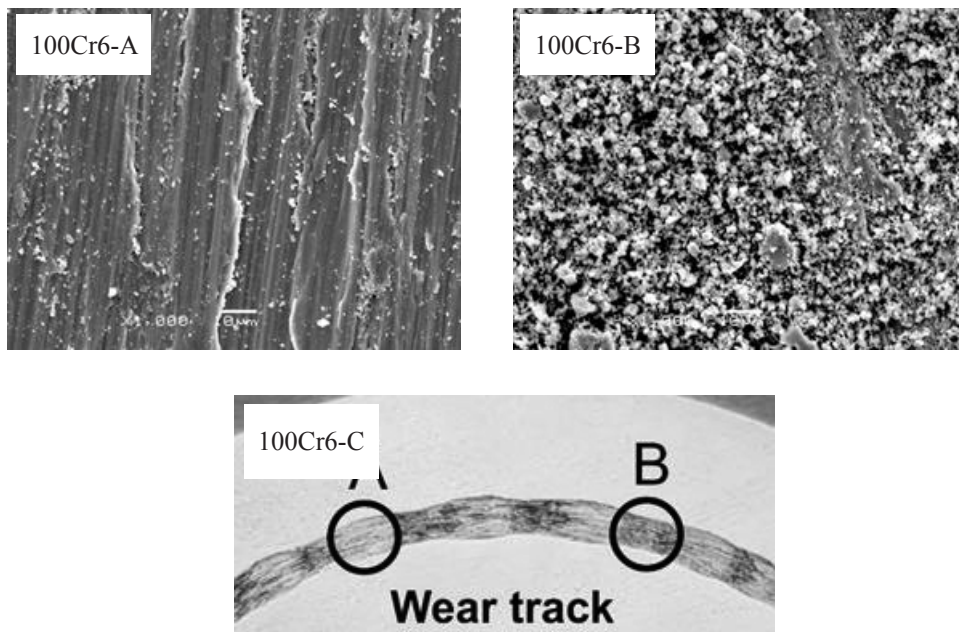


**Fig. 11. Surface of the wear trace on a Ti-6Al-7Nb sample in the non-oxidized condition with visible corrugation wear after interaction with a 100Cr6 ball (Fig. a – area with a trace amount of wear products, b – area with densely located wear products, c – macroscopic view of the wear trace with marked areas “a” and “b”)**

Rys. 11. Powierzchnia śladu zużycia na próbce ze stopu Ti-6Al-7Nb w stanie nieutlenionym z widocznym zużyciem falistym po współpracy z kulką 100Cr6 (rys. a – obszar ze śladową ilością produktów zużycia, b – obszar z gęsto ulokowanymi produktami zużycia, c – widok makroskopowy śladu zużycia wraz z zaznaczonymi obszarami „a” i „b”)

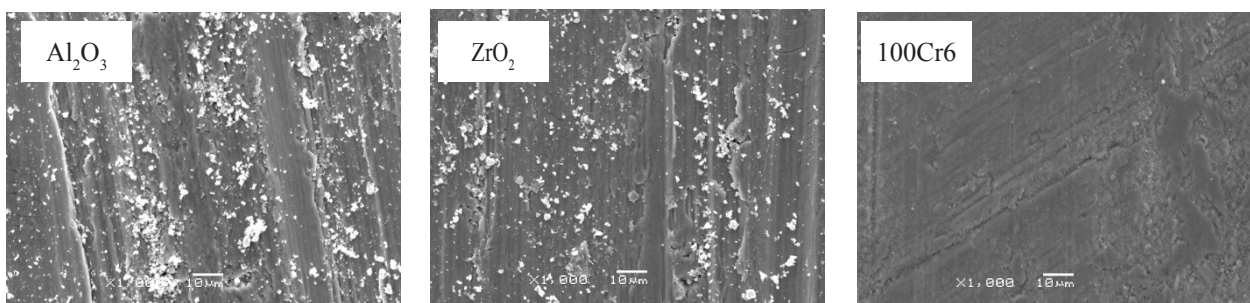


**Fig. 12. Surface of the wear trace on Ti-6Al-7Nb samples oxidized at 600°C after interaction with  $\text{Al}_2\text{O}_3$ ,  $\text{ZrO}_2$  and 100Cr6 balls**

Rys. 12. Powierzchnia śladu zużycia na próbkach ze stopu Ti-6Al-7Nb w stanie utlenionym w temperaturze 600°C po współpracy z kulkami  $\text{Al}_2\text{O}_3$ ,  $\text{ZrO}_2$  oraz 100Cr6

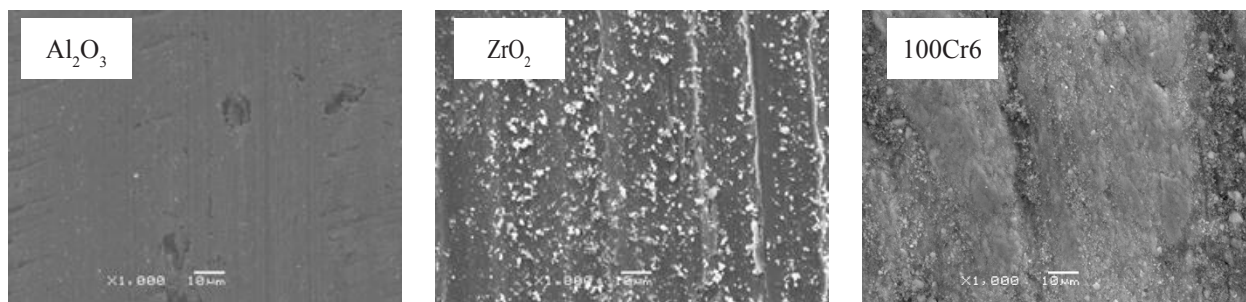


**Fig. 13.** Surface of the wear trace on Ti-6Al-7Nb samples oxidized at 650°C after interaction with Al<sub>2</sub>O<sub>3</sub>, ZrO<sub>2</sub>, and 100Cr6 balls

Rys. 13. Powierzchnia śladu zużycia na próbkach ze stopu Ti-6Al-7Nb w stanie utlenionym w temperaturze 650°C po współpracy z kulkami Al<sub>2</sub>O<sub>3</sub>, ZrO<sub>2</sub> oraz 100Cr6

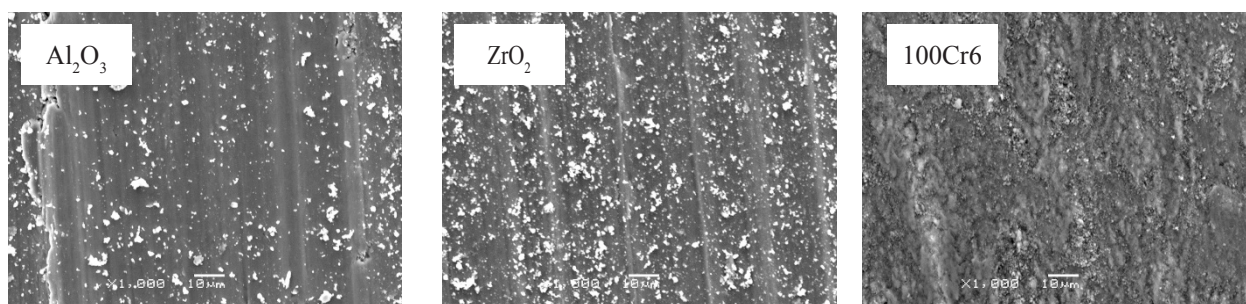


**Fig. 14.** Surface of the wear trace on Ti-6Al-7Nb samples oxidized at 700°C after interaction with Al<sub>2</sub>O<sub>3</sub>, ZrO<sub>2</sub> and 100Cr6 balls

Rys. 14. Powierzchnia śladu zużycia na próbkach ze stopu Ti-6Al-7Nb w stanie utlenionym w temperaturze 700°C po współpracy z kulkami Al<sub>2</sub>O<sub>3</sub>, ZrO<sub>2</sub> oraz 100Cr6

Based on the observations, a diverse morphology of the friction surface was found after tribological tests. On the non-oxidized samples, after the interaction with Al<sub>2</sub>O<sub>3</sub> and ZrO<sub>2</sub> balls, a similar morphology of the working surface was observed, with scratches formed as a result of friction and fine wear products of oxide origin. After the tribological interaction with the 100Cr6 bearing steel, “corrugation wear” was observed, as distinguished by the presence of characteristic, alternate dark and light areas (Fig. 11c). The observed areas clearly differed in their surface morphologies. The surface of dark areas was densely covered with products of tribological wear (Fig. 11b), while, on the light colour area, trace amounts of wear products were found (Fig. 11a). Tests have shown that isothermal oxidation eliminates this disadvantageous phenomenon completely. After isothermal oxidation at 600, 650, and 700°C, scratches were observed on the surface of the investigated alloy, which formed after the tribological interaction with Al<sub>2</sub>O<sub>3</sub> and ZrO<sub>2</sub> balls, with a small amount of wear products (Figs. 12 to 14a and b). A completely different morphology was found after interaction with 100Cr6 balls (Figs. 12–14c). The observed surfaces did not show any scratches and their morphology was similar to oxide layers, which indicates that the working surface of friction got oxidized during the tribological tests.

## CONCLUSIONS

Based on the performed research and analysis of its results, the influence was determined of isothermal oxidation parameters and of the friction couple on tribological properties of the Ti-6Al-7Nb alloy. The following conclusions have been formulated:

1. Thermal oxidation conducted at temperatures of 600°C, 650°C, and 700°C enables obtaining good-quality oxide layers with diverse morphologies and tribological properties.
2. In the study, after oxidation at 600°C and 650°C, a uniform oxide layer was obtained on the surface of the Ti-6Al-7Nb alloy, which concentrated mostly on the roughness elevations formed during the grinding of specimens. An increase in the oxidation temperature to 700°C led to obtaining an oxide layer with local concentrations of fine oxide particles.
3. Oxide layers obtained on the surface of alloy Ti-6Al-7Nb induced a significant increase in the friction coefficient.
4. The surface of alloy Ti-6Al-7Nb after isothermal oxidation showed more advantageous tribological properties. The best resistance to sliding wear was shown by the oxide layer obtained at 650°C. The reason for the significant improvement of tribological



properties was the presence of oxide layers of high hardness on the surface of the investigated alloy.

5. SEM observations of traces of wear revealed the presence of numerous scratches and fine wear products on the friction surface. For the non-oxidized

condition, after interaction with a 100Cr6 ball, the presence was found of alternating, morphologically varied areas which had formed as a result of corrugation wear. It was shown that oxide layers eliminate this unfavourable phenomenon.

## REFERENCES

1. Wang S., Liao Z., Liu Y., Liu W.: Influence of thermal oxidation duration on the microstructure and fretting wear behavior of Ti6Al4V alloy. *Materials Chemistry and Physics* 159 (2015), pp. 139–151.
2. Guleryuz H., Cimenoglu H.: Oxidation of Ti–6Al–4V alloy. *Journal of Alloys and Compounds* 472 (2009), pp. 241–246.
3. Li L., Yu K., Zhang K., Liu Y.: Study of Ti–6Al–4V alloy spectral emissivity characteristics during thermal oxidation process. *International Journal of Heat and Mass Transfer* 101 (2016), pp. 699–706.
4. Fellah M., Assala O., Labaiz M., Dekhil L., Iost A.: Friction and Wear Behavior of Ti-6Al-7Nb Biomaterial Alloy. *Journal of Biomaterials and Nanobiotechnology* 4 (2013), pp. 374–384.
5. Ahn H., Lee D., Lee K-M., Lee K., Baek D., Park S-W.: Oxidation behavior and corrosion resistance of Ti–10Ta–10Nb alloy. *Surface & Coatings Technology* 202 (2008), pp. 5784–5789.
6. Gilbert J.L., Buckley C.A., Lautenschlager E.P.: Titanium oxide film fracture and repassivation: The effect of potential, pH and aeration. In: Brown S.A., Lemons J.E., editors. *Medical applications of titanium and its alloys: the material and biological issues*, ASTM STP 1272. Philadelphia: ASTM; 1996, pp. 199–214.
7. Long M., Rack H.J.: Titanium alloys in total joint replacement a material science perspective, *Biomaterials* 19 (1998), pp. 1621–1639.
8. Li L., Yu K., Zhang K., Liu Y.: Study of Ti–6Al–4V alloy spectral emissivity characteristics during thermal oxidation process. *International Journal of Heat and Mass Transfer* 101 (2016), pp. 699–706.
9. Aniołek K., Kupka M., Łuczuk M., Barylski A.: Isothermal oxidation of Ti-6Al-7Nb alloy. *Vacuum* 114 (2015), pp. 114–118.
10. Kumar S., Narayanan T.S.N.S., Raman S.G.S., Seshadri S.K.: Thermal oxidation of Ti6Al4V alloy: microstructural and electrochemical characterization. *Materials Chemistry and Physics* 119 (2010), pp. 337–346.
11. Wang S., Liao Z., Liu Y., Liu W.: Influence of thermal oxidation temperature on the microstructural and tribological behavior of Ti6Al4V alloy. *Surface & Coatings Technology* 240 (2014), pp. 470–477.
12. Dearnley P.A., Dahm K.L., Çimenoglu H.: The corrosion–wear behaviour of thermally oxidised CP-Ti and Ti–6Al–4V. *Wear* 256 (2004), pp. 469–479.
13. Arslan E., Totik Y., Demirci E., Alasaran A.: Influence of Surface Roughness on Corrosion and Tribological Behavior of CP-Ti After Thermal Oxidation Treatment. *Journal of Materials Engineering and Performance* 19 (2010), pp. 428–433.